# A COMPARATIVE STUDY OF OXYGEN VACANCY MIGRATION PATHWAYS IN CRYSTALLINE POLYMORPHS OF SILICA

L. René Corrales

Pacific Northwest National Laboratory
Richland, WA 99352
Corresponding author:
rene.corrales@pnl.gov

Hannes Jónsson

Department of Chemistry
University of Washington
Seattle, WA 98195

Jakyoung Song
and
Renée M. VanGinhoven

Pacific Northwest National Laboratory
Richland, WA 99352
and
Department of Chemistry
University of Washington
Seattle, WA 98195

## ABSTRACT

The migration pathway and energy of an oxygen vacancy were calculated in quartz, stishovite and cristobolite using an empirical potential. For comparison the minimum energy pathway in quartz was calculated using density functional theory. The differences between the two methods show that although the energies of both approaches are similar, the pathways go through different intermediate states and, hence, the mechanisms of diffusion would appear to be different.

## INTRODUCTION

The migration of an oxygen vacancy is responsible for ionic conduction in oxide insulators and is also associated with the aggregation of voids to form bubbles in irradiated ceramics and glasses.[1] Many studies are being carried out to study the migration energetics using empirical model potentials.[2] However, defects in oxide networked materials come in various "flavors".[1] Some are neutral radicals, some are charged states and still others are a mixture of these, such as the E' center in silica. One issue in the use of empirical potentials is that they do not capture the electronic response to the formation of defects and their migration.[3] The extent to which empirical models are deficient is not well characterized. It is, therefore, useful to determine the nuances that may plague the use of empirical potentials when used to study the migration of defects. One

approach is to compare similar sets of empirical potential calculations with ab initio calculations. In this work, we have calculated the migration pathways of the oxygen vacancy in quartz using density functional theory (DFT)[4] and compared those results with pathways calculated using the empirical potential of van Beest, Kramer and van Santen (the BKS potential).[5] The initial starting pathways used in the DFT calculations were obtained with the assistance of the BKS potential. The oxygen vacancy migration pathways are calculated for stishovite and cristobolite using the BKS potential. The pathways were determined using the nudged-elastic band (NEB)[6] method that was coupled with both the DFT and the BKS potentials.

## THEORETICAL MODELS AND METHODS

### Density Functional Theory

In this work, the DFT calculations were carried out using VASP[7] (Vienna ab initio simulation program. VASP is a plane wave DFT code based on local-density approximation (LDA) and generalized gradient corrections (GGC) in the Perdew-Wang 91 approximation. In addition, the ultrasoft Vanderbilt pseudopotential (USPP) and spin polarization were used. The energy cutoffs were 29 Ry for the wave functions and 68 Ry for the augmented electron density. The Brillouin zone of the cell was sampled only at the Γ point. The system consisted of 72 atoms made up of 24 silicon and 48 oxygen atoms in a periodic orthorhombic cell. Optimization of the structures was carried out using an iterative conjugate gradient minimization scheme.

### BKS Potential Molecular Dynamics

The BKS potential is a Coulombic potential that includes a modified Buckingham potential for the repulsion and dispersion interactions, respectively, that is given by

$$E = \sum_{i>j}\left[A_{ij}\exp\left(-b_{ij}r_{ij}\right) - \frac{C_{ij}}{r_{ij}^{6}}\right] + \sum_{i>j}\frac{q_i q_j}{r_{ij}} \qquad (1)$$

where $r_{ij}$ is the distance between atoms i and j, the parameter $A_{ij}$, $b_{ij}$, and $C_{ij}$ are fit to ab initio and empirical data, and the $q_i$ are fixed partial charges of the atoms as determined from ab initio calculations of a tetrahedral silica cluster.[5] The parameters used in this work are listed in Table 1. The Coulombic interaction is between all atom pairs, whereas the exp-6 interaction is only between Si-O and O-O atom pairs. A harmonic function is added to the potential function for r less than 1.1936 Å and 1.439Å for the Si-O and O-O interactions, respectively, because of the low energy barrier at small r due to the dominance of the exponential term. Thus, a repulsive interaction at small r is maintained, which is generally required for high temperature simulations and is also necessary when

determining the diffusion pathways of the atoms. This prevents the pathological fusion of the atoms that could otherwise occur.

Table I. Parameter set for BKS potential

| Atom pair | $A_{ij}$ (eV) | $b_{ij}$(Å$^{-1}$) | $C_{ij}$ (eV Å$^6$) | Charges |
|---|---|---|---|---|
| **O-O** | 1388.773 | 2.760 | 175.000 | $q_O = -1.2$ |
| **Si-O** | 18003.757 | 4.873 | 33.538 | $q_{Si} = +2.4$ |

In this work, the potential is implemented in a MD computer simulation code using Ewald sums for the long range Coulomb interaction. Minimization of a structure is carried out using a velocity Verlet algorithm in which each simulation is started at zero velocity. Atoms that are not at the potential minimum slide down the potential well and gain velocity. As they turn around at the minimum the velocity reaches a maximum. At this point, the velocities are reset to zero and the simulation continued until a zero velocity convergence is reached.

The $\alpha$-quartz lattice is generated using orthogonal periodic boundary conditions. The vacancy was introduced and the structure relaxed using a system size of 576 atoms of stoichiometric makeup. The cristobolite and stishovite lattices also consisted of 576 atoms and were relaxed using orthogonal periodic boundary conditions.

The Nudged-Elastic Band Method

In the NEB method,[8] a chain of images, representing molecular configurations, is "strung" along a probable path where endpoints are either well-characterized defect points, or a good guess for defect localization. Springs with a specified force, or spring constant, couple each of the nearest neighbor images. For each image, the forces of the atoms are calculated. The forces due to the spring constants are added to the corresponding atomic forces of the image, and hence the images are coupled via the spring force contributions. Certain constraints must be applied to prevent, for example, the chain from bunching up on either side of a peak near a steep incline, where they slide off the incline and completely cut off the peak. The stiffness of the springs can also lead to the images climbing up the walls of the potential leading to corner cutting. Introducing the "nudging" technique prevents the corner cutting and slide-off problems. The nudging technique is implemented by setting the spring force perpendicular to the path to zero, while maintaining the forces parallel to the path. At the same time, forces due to the potential that are parallel to the path are set to zero, while maintaining those forces perpendicular to the path. This keeps the images equally spaced along the path. The resolution of the path can be improved

by providing more images, or by reducing the path length of the images. This method is very fast and efficient, nominally converging in 100 time steps using an MD optimization method, depending on path length, number of images, complexity of the potential and size of the system. The method scales as the time required for a single image multiplied by the number of images, where for empirical potentials the single image scales as $N^2$, where N is the number of atoms in the simulation box. This method calculates the paths of the defect migration while locating the barriers and local minima along the path.

## RESULTS

First, the migration pathway and energetics of the charged oxygen vacancy in α-quartz between the DFT and the empirical BKS potentials are compared. Both sets of calculations were carried out using the NEB method. The BKS potential

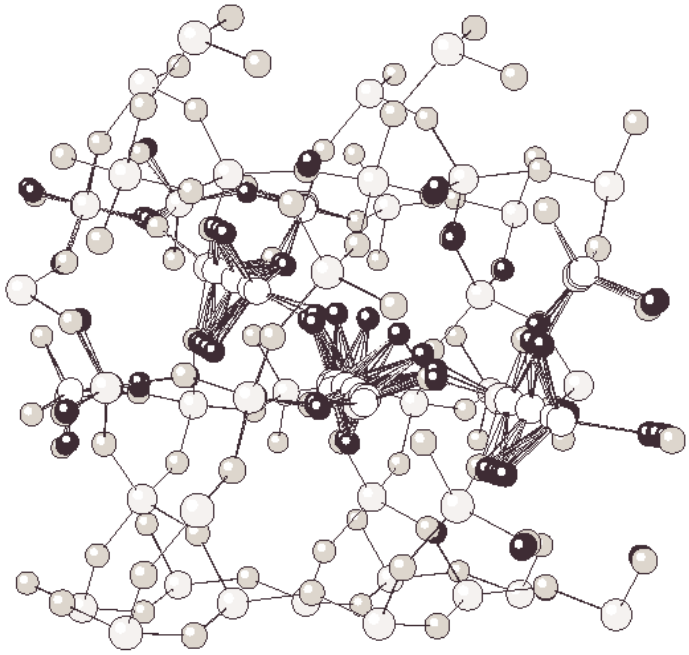

**Figure 1**. The migration of an oxygen atom in quartz calculated using the BKS potential. The dark gray atoms are the oxygens, the light gray atoms are the silicons, the black atoms are the migrating (or relaxing) oxygens and the white atoms are the migrating silicon atoms. As the oxygen migrates, one silicon atom moves from the puckered position to a bonded state, while another silicon moves from the bonded state to a puckered position. Hence, several atoms are involved in the migration process.

can only model charged states, and even then only the oxygen vacancy with a partial charge of +1.2. The DFT method does not limit the charge state of the atoms. In this study an oxygen atom and an electron are removed from the initial system, to create a vacancy with a charge of +1. The difference between the two methods is that the BKS potential predicts only a puckered configuration, whereas the DFT method predicts both a planar and a puckered configuration. The latter is in agreement with previous ab initio[9] and other DFT calculations.[10] For the NEB calculations, the initial and final states for the BKS potential are puckered states, and the initial and final states for the DFT method are the planar states.

The migration of the vacancy is effectively the migration of an oxygen atom from one given site to the vacancy site. Hence, several nearest neighbor oxygen atoms can diffuse to the vacancy. In Figure 1, an image of the quartz configuration using the BKS potential is shown. This particular image does not depict the lowest energy pathway, but illustrates how numerous atoms shift

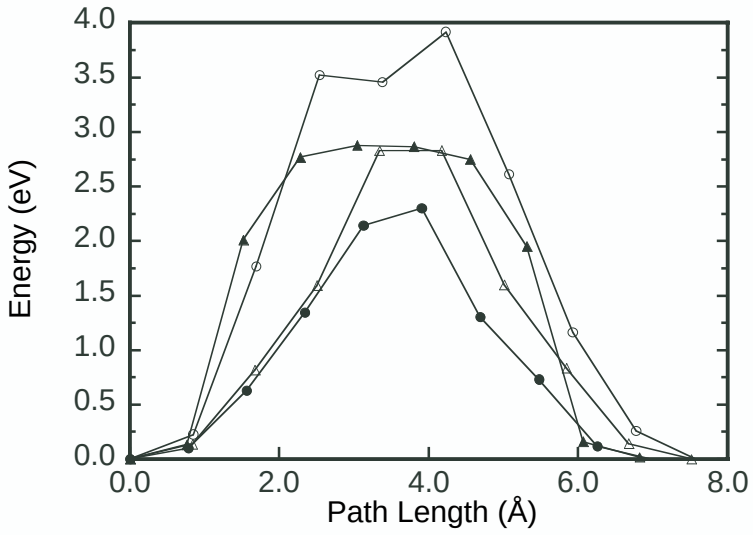


**Figure 2**. Energy versus path length along migration pathway of several different near neighbor oxygen atoms determined using 10 images in the calculation. Each distinct path and barrier energy is from oxygen atoms from distinct initial positions. In general, oxygen atoms in starting positions closer to the vacancy, or that need to maneuver around fewer atoms, have lower energy barriers to migration into the vacancy. The lowest barrier pathway, marked with filled circles, is the path used to provide a starting path for the DFT calculation.

positions along with the migrating oxygen. As the oxygen atom moves toward the vacancy, the silicon atom in the puckered position begins to move into the regular bonded position, while another silicon atom moves out of the regular bonded position into the puckered position.

Many pathways can be investigated using the BKS potential. From these calculations, the configuration and energy of the transition state can be determined. The energies of some of these pathways are shown in Figure 2. The pathway calculations vary from 1/2 to 8 CPU hours on an SGI Origin 2000, depending upon the system size, the number of images, convergence criterion, path length and proximity of the initial guess path to the final calculated path.

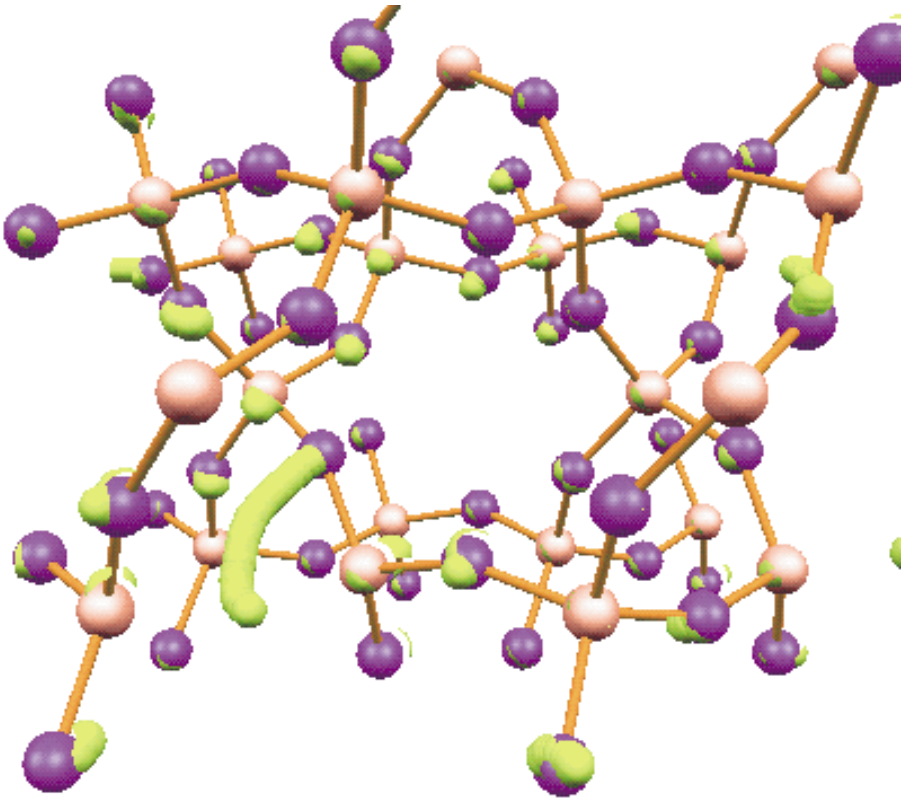

**Figure 3**. The migration of an oxygen atom in quartz determined using the DFT method. The initial and final states of the silicon atoms adjacent to the vacancy are in the planar state. In contrast to the migration using the BKS potential, the motion of the surrounding atoms is minimal. The dark gray atoms are the oxygen atoms, the medium gray atoms are the silicon atoms, and the light gray atom is the migrating oxygen.

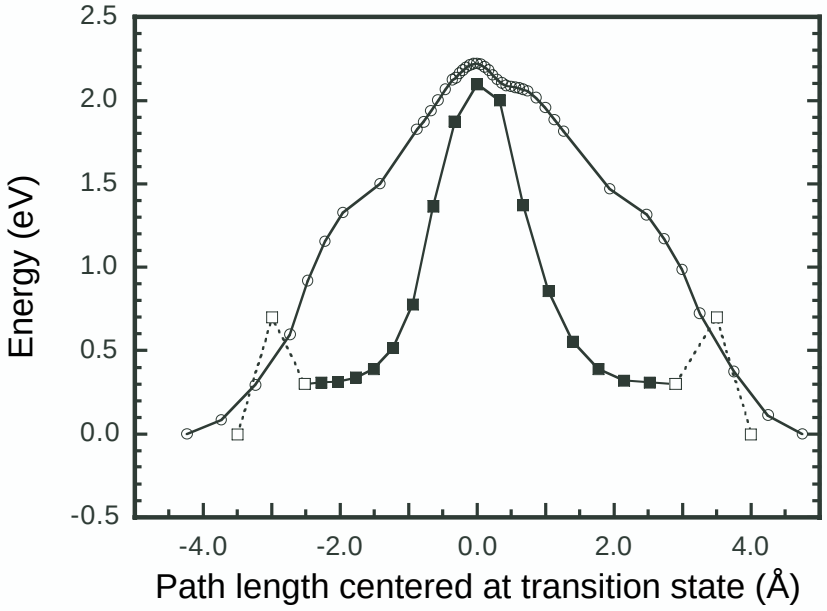


**Figure 4**. The lowest energy migration pathway of the oxygen vacancy determined in quartz. The curve with the filled squares was calculated using DFT. The curve with the open circles was calculated using the BKS potential. The total path length is a measure of all the atoms that are moving and relaxing. The dotted lines with open squares are a schematic of the transition from the puckered to planar state predicted by DFT. The number of images using the BKS potential was increased near the transition state to increase the resolution.

The lowest energy pathway determined using the BKS potential was used as a guide to choose the initial path configuration for the DFT calculation. It is useful to have a starting path configuration because the DFT calculations require up to 5000 CPU node hours on an IBM SP2 for the 16 image calculations. The minimum energy pathway for the oxygen vacancy migration in quartz determined by the DFT method is shown in Figure 3.

In Figure 4, the minimum energy migration pathway of the DFT calculation is compared with the minimum energy pathway of the BKS potential. The pathway predicted by the BKS potential is from a puckered state to another puckered state. The DFT calculation predicts that the oxygen vacancy migrates through an intermediate planar state on each side of the transition state. Other DFT calculations[10], as well as our own, show that there is a planar and a puckered state of the silicon atoms that are adjacent to the oxygen vacancy. Thus, in Figure 4, the total path from puckered state to puckered state can be compared to the empirical potential result by adding in this additional pathway to the DFT result. The planar

state is found to be 0.3 eV higher in energy than the puckered state. Boero et. al. have determined a barrier energy of 0.7 eV[10] to go from the puckered state to the planar state. The motion mostly involves one silicon atom. Our calculations show

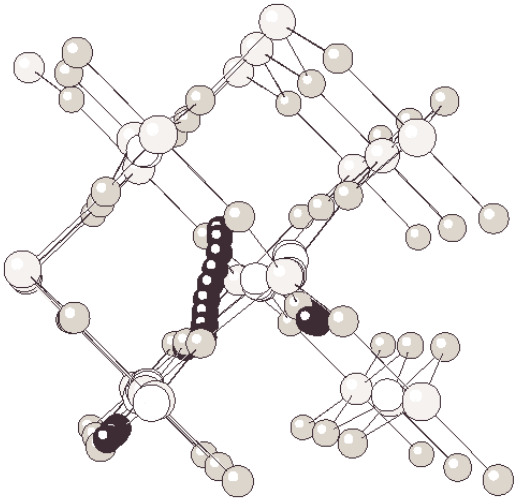

**Figure 5**. The migration of an oxygen atom in stishovite determined using the BKS potential. The shading scheme is identical to that in Figure 1. As the oxygen migrates, fewer atoms are involved in the migration process with significantly less relaxation of the network, as compared to quartz.

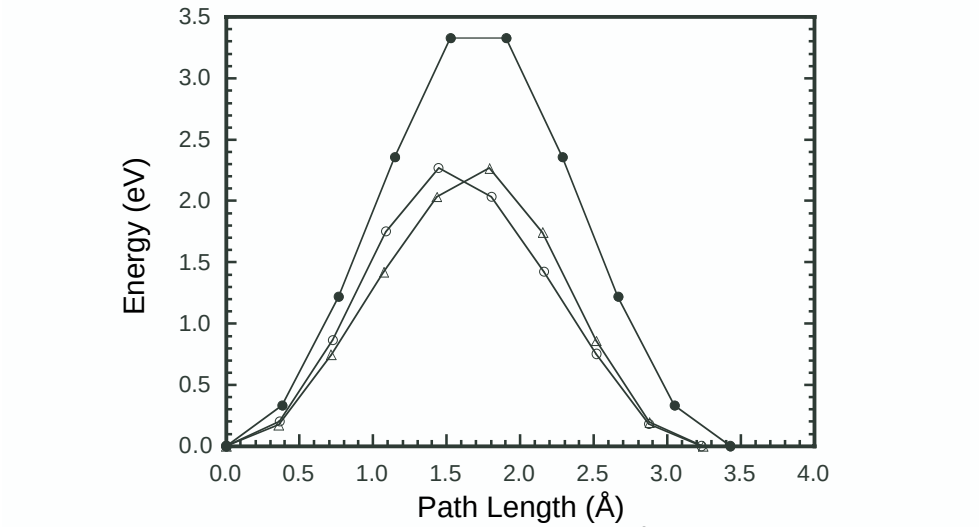


**Figure 6**. The migration path lengths and energetics of an oxygen atom in stishovite calculated using the BKS potential. The packing in stishovite is such that the nearest neighbors only show an exchange (not shown) and it is the next-nearest neighbors that lead to migration.

that the oxygen vacancy migrates from a planar state to another planar state occurs with a barrier energy of 1.8 eV. The overall barrier for vacancy migration using DFT is 2.1 eV. The migration barrier energy determined by the BKS potential is 2.2 eV. However, the BKS potential pathway never goes through a minimum (meta-stable) configuration in the planar state. So although the barrier energies appear to be similar, there are substantial differences in the mechanisms that may affect the underlying diffusion kinetics.

The migration of an oxygen vacancy for the stishovite crystal is shown in Figure 5. This particular crystal phase does not show a rearrangement of the silicon atoms to a "puckered" configuration as observed in the BKS calculation of quartz. This is because the silicon atoms adjacent to the vacancies are already bonded to a back oxygen atom. However, in the presence of the vacancy the bond length between the silicon and the back oxygen is shortened. Hence, there is less motion of the silicon atoms adjacent to the migrating oxygen atom. Several paths were investigated of which some are shown in Figure 6.

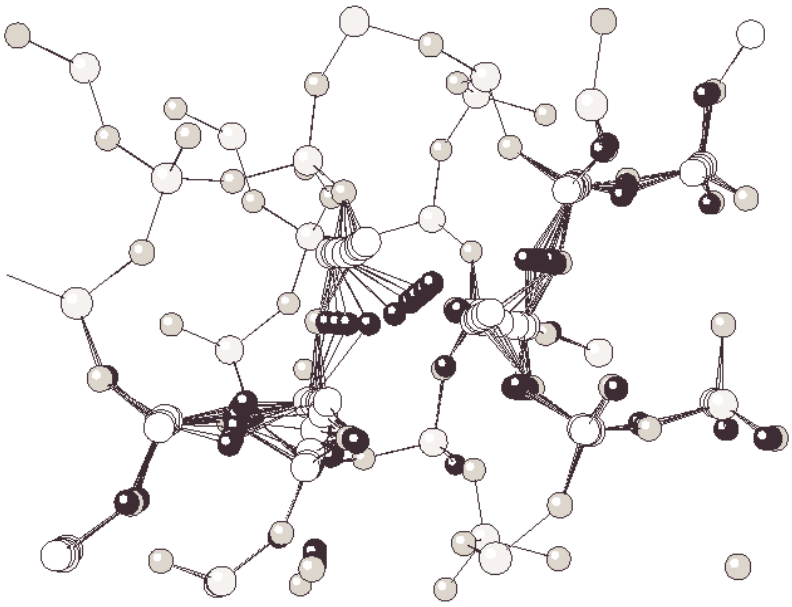

**Figure 7**. The migration of an oxygen atom in cristobolite determined using the BKS potential. The shading scheme is identical to that in Figure 1. As the oxygen migrates, one silicon atom moves from the puckered position to a bonded state, while another silicon moves from the bonded state to a puckered position. Hence, several atoms are involved in the migration process.

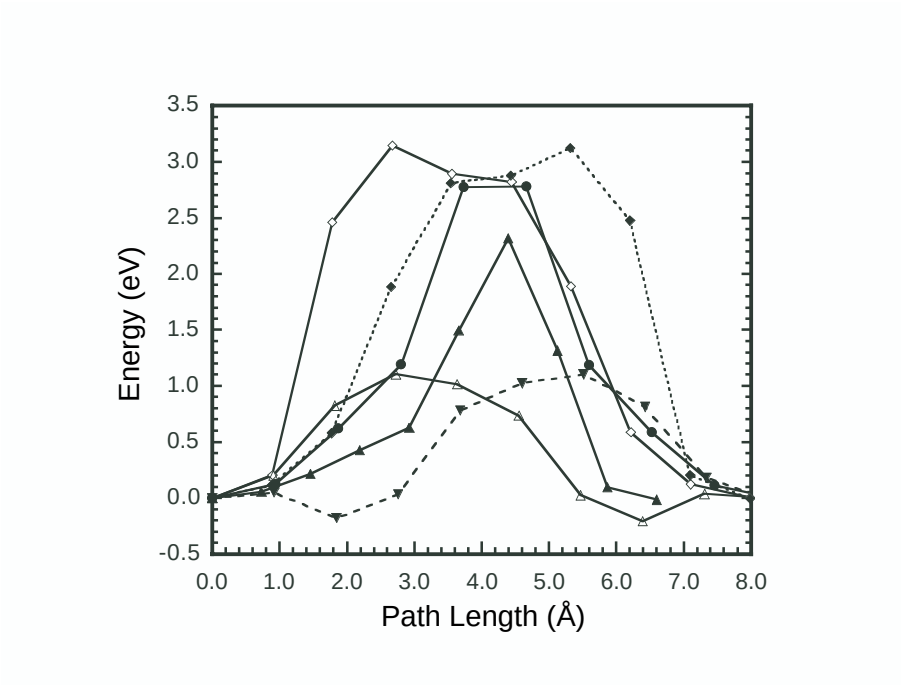


**Figure 8**. The migration path lengths and energetics of an oxygen atom in cristobolite calculated using the BKS potential. The negative energies are due to the preferred relaxed state of the oxygen vacancy for that particular path, the closed and open triangles. The "mirror" paths are equivalent paths that are traversed in opposite directions. This occurs when the crystal symmetry of the vacancy preserves the original symmetry of the crystal.

The migration of an oxygen vacancy for the cristobolite crystal is shown in Figure 7. This particular crystal phase also shows a rearrangement of the silicon atoms to a "puckered" configuration as observed in the BKS calculation of quartz. There is significant motion of silicon atoms adjacent to the vacancy, as well as relaxation of several network atoms as the oxygen atom migrates. Several of the paths investigated are shown in Figure 8. In this figure, we have shown paths that "mirror" each other. Such paths also exist in quartz and stishovite, but were not shown in their respective path length plots.

## DISCUSSION

The migration pathway calculations of the oxygen vacancy in quartz show similar energetics for the barrier energy using DFT and the BKS potentials. However, there are clearly differences in the underlying diffusion mechanism. The BKS potential has a puckered structure for the initial and final states of the vacancy defect. DFT also predicts the puckered configuration as the lowest energy state, but also shows that there is a barrier of 0.4 eV between it and a metastable planar configuration. The paths appear to be quite similar at the transition state, even though the BKS potential does not predict a meta-stable intermediate state. The BKS transition state is observed to occur a little earlier

along the path. This is determined by measuring the distances between the silicon atoms bonded to the migrating oxygen atom. During the migration, the silicon atoms initially bonded to the oxygen move away from each other, while the atoms finally bonded to the oxygen move closer together. At the transition state, the distance between the initial silicon atoms is 3.10 Å for the BKS potential, and 3.44 Å for DFT. The distance between the two final silicon atoms is 3.22 Å and 2.80 Å for the BKS and DFT transition states, respectively. When comparing these distances, it is important to keep in mind that the silicon – silicon near neighbor distance in the perfect crystal is 3.08 Å and 3.12 Å for the BKS and DFT methods, respectively.

The migration pathway calculations in stishovite and cristobolite reveal similarities and differences when compared to the quartz calculations. These were calculated using only the BKS potential. The existence of backbonding structures, which is a signature of the puckered configuration, persists in all three crystalline structures. It would thus be valuable to carry out more detailed DFT calculations of the vacancy defect in these crystal structures to determine the stable and meta-stable structures, as in quartz.

## CONCLUSION

The migration pathway of an oxygen vacancy was calculated in quartz using both DFT and the BKS potentials. The BKS potential was also used to calculate the pathways in stishovite and cristobolite. The results show that although the transition state determined by both methods are similar, the pathways at the endpoints are not the same. It may be that a model potential that includes electronic response of the atoms would give a path more similar to the DFT result. Finally, it is important to determine the details of the underlying migration pathway, in addition to the barrier energies, to gain a fundamental understanding of how atomic level diffusion of vacancy defects manifest in the collective behavior of bubble formation in nuclear waste materials.

## ACKNOWLEDGEMENT

The DFT calculations have been performed using the ab-initio total-energy and molecular dynamics program VASP (Vienna ab-initio simulation program) developed at the Institut für Theoretische Physik of the Technische Universität Wien.[7] This work was supported by (JS and RMV) the Environmental Management Science Program, Office of Environmental Management, U.S. Department of Energy and by (LRC) the Division of Chemical Sciences, Office of Basic Energy Sciences, Department of Energy. This research was performed in the William R. Wiley Environmental Molecular Sciences Laboratory, a national scientific user facility sponsored by the Department of Energy's Office of Biological and Environmental Research and located at Pacific Northwest National Laboratory. Pacific Northwest National Laboratory is operated for the Department of Energy by Battelle.

**REFERENCES**


1 W. J. Weber, R. C. Ewing, C. A. Angell, G. W. Arnold, A. N. Cormack, J. M. Delaye, D. L. Griscom, L. W. Hobbs, A. Navrotsky, D. L. Price, A. M. Stoneham and M. C. Weinberg, Radiation effects in glasses used for immobilization of high-level waste and plutonium disposition, J. Mater. Res., Vol. 12, No. 8, 1946-1978 (1997).

2 For example: P. J. Wilde and C. R. A. Catlow, Defects and diffusion in pyrochlore structural oxides, Solid State Ionics 112 (1998) 173-183; and R. E. Williford, R. Devanathan and W. J. Weber, Computer simulations of displacement energies for several ceramic materials, Nucl. Instrum. and Meth. B 141 (1998) 94-98.

3 A. Chen and L. R. Corrales, A semi-empirical methodology to simulate silica: Ionic and atomistic dissociation, J. Non-Cryst. Solids (in press).

4 P. Hohenberg and W. Kohn, Inhomogenuous electron gas, Phys. Rev. 136 (1964) B864 – B871; W. Kohn and L. J. Sham, Self-consistent equations including exchange and correlation effects, Phys. Rev. 140 (1965) A1133 – A1138; R. Carr and M. Parrinello, Unified approach for molecular dynamics and density-functional theory, Phys. Rev. Letters, 55, 2471 (1985); K. Laasonen, R. Car, C. Lee and D. Vanderbilt, Implementation of ultrasoft pseudopotentials in ab initio moecular dynamics, Phys. Rev. B 43 (1991) 6796-6799.

5 B. W. H. van Beest, G. J. Kramer and R. A. van Santen, Force fields for silicas and aluminophosphates based on ab initio calculations, Phys. Rev. Lett. 64 (16), 1955-1958 (1990); G.J. Kramer, N.P. Farragher, B.W.H. van Beest and R.A. van Santen,Interatomic force fields for silicas, aluminophosphates, and zeolites: Derivation based on ab initio calculations, Phys. Rev. B 43 (6), 5068-5080 (1991).

6 H. Jonsson, G. Mills, and W. Jacobsen, Nudged elastic band method for finding minimum energy paths of transitions, in Classical and Quantum Dynamics in Condensed Phase Simulations, B.J. Berne, G. Cicotti and D.F. Coker, editors (World Scientific, 1998).

7 G. Kresse and J. Hafner, Ab initio molecular dynamics for liquid metals, Phys. Rev. B 47 (1), 558-561 (1993); G. Kresse and J. Hafner, Ab initio molecular dynamics simulations of the liquid metal amorphous-semiconductor transition in germanium, Phys. Rev. B 49 (1994) 14251; G. Kresse and J. Furthmüller, Comput. Mat. Sci. 6, 15 (1996); G. Kresse and J. Furthmüller, Efficient iterative schemes for ab initio total-energy calculations using a plane-wave basis set, Phys. Rev. B 54 (16) 11169-11186 (1996).

8 G. Mills, H. Jónsson and G. K. Schenter, Reversible work transition state theory: application to dissociative adsorption of hydrogen, Surf. Sci. 324 (1995) 305-337.

9 W. B. Fowler and A. H. Edwards, Theory of defects and defect processes in silicon dioxide, J. Non-Cryst. Solids, 222, 33-41 (1997); and references therein.

10 M. Boero, A. Pasquarrello, J. Sarnthein and R. Car, Structure and hyperfine parameters of $E'_1$ centers in $\alpha$-quartz and in vitreous $SiO_2$, Phys. Rev. Letters 78 (1997) 887.